Received: 23 October 2025 | Revised: 1 April 2026 | Accepted: 5 April 2026

DOI: 10.1111/bph.70479

RESEARCH ARTICLE

Contact sensitisers activate keratinocytes and induce cytotoxicity via Transient Receptor Potential Ankyrin 1 in allergic contact dermatitis

Areej Jaber[1,2] | Szabina Horváth[2] | Balázs Zoltán Zsidó[1] | Viktória Kormos[1] | János Konkoly[1] | Csaba Hetényi[1] | Erika Pintér[1] | Ágnes Kemény[1,3] | Rolland Gyulai[2,4]

[1]Department of Pharmacology and Pharmacotherapy, Medical School, University of Pécs, Pécs, Hungary

[2]Department of Dermatology, Venereology, and Oncodermatology, Medical School, University of Pécs, Pécs, Hungary

[3]Department of Physiology and Biochemistry, University of Veterinary Medicine, Budapest, Hungary

[4]Department of Dermatology and Allergology, Albert Szent-Györgyi Faculty of Medicine, University of Szeged, Szeged, Hungary

Correspondence
Areej Jaber, Department of Pharmacology and Pharmacotherapy and Department of Dermatology, Venereology, and Oncodermatology, Medical School, University of Pécs, 7624 Pécs, Hungary.
Email: jaber.areej@pte.hu

Funding information
This work was supported by the Ministry for Innovation and Technology of Hungary through the TKP2021-EGA-16 and TKP2021-EGA-10 grant programmes and by the Hungarian Brain Research Program (NAP-3), provided through the HUN-REN. V. K. was supported by the Research grant of Medical School, University of Pécs (008_2025_PTE_RK/36). B. Z. Zs. was supported by the János Bolyai Research Scholarship of the Hungarian Academy of Sciences (BO/00189/24/5).

Abstract

Background and Purpose: Allergic contact dermatitis (ACD) is a frequent inflammatory skin disease with limited therapeutic options. While neuronal Transient Receptor Potential Ankyrin 1 (TRPA1) has been implicated in ACD, the role of keratinocyte TRPA1 remains unclear. We investigated whether allergen binding to keratinocyte TRPA1 drives cytotoxicity, cytokine release and inflammatory amplification.

Experimental Approach: We combined *in vivo* oxazolone-induced hypersensitivity in wild-type and *Trpa1* knockout mice with pharmacological inhibition by HC-030031, *in vitro* assays using TRPA1-expressing Chinese hamster ovary (CHO) cells and primary keratinocytes, RNAscope localisation in human and murine skin, cytokine profiling and *in silico* docking analyses of allergen-TRPA1 interactions.

Key Results: TRPA1 deletion or antagonism markedly reduced oxazolone-induced ear swelling, vascular responses and histopathology. Strong contact sensitisers (2,4-dinitrochlorobenzene [DNCB], 2,4-dinitrofluorobenzene [DNFB], oxazolone and formaldehyde) activated TRPA1, inducing Ca^{2+} influx, cytotoxicity and IL-1α release, effects absent in *Trpa1*-deficient cells and inhibited by HC-030031. RNAscope confirmed keratinocyte TRPA1 expression in human and mouse skin. Docking revealed allergen-specific binding modes, where covalent cysteine modification and A-loop stabilisation correlated with potency. Consistent with these observations allergen-induced ROS, which also target the cysteine cluster of TRPA1, may further lower the channel's activation threshold and thereby amplify allergen-driven cytotoxicity.

Conclusion and Implications: Keratinocyte TRPA1 integrates direct allergen binding with ROS-mediated sensitisation to drive cytotoxicity and IL-1α release. This dual mechanism helps explain sensitiser potency and positions TRPA1 antagonism as a

Abbreviations: ACD, allergic contact dermatitis; CHO, chinese hamster ovary; DNCB, 2,4-dinitrochlorobenzene; DNFB, 2,4-dinitrofluorobenzene; ECS, extracellular solution; HC, HC-030031 (selective TRPA1 antagonist); MCP-1, monocyte chemoattractant protein-1; MO, allyl isothiocyanate (mustard oil; TRPA1 agonist); Trpa1 (mouse gene) / TRPA1 (protein), Transient receptor potential ankyrin 1.

Erika Pintér, Ágnes Kemény and Rolland Gyulai contributed equally to this work and share last authorship.

promising therapeutic approach in ACD, while providing a framework for chemical risk assessment.

KEYWORDS
allergic contact dermatitis, electrophilic allergens, HC-030031 [HC030031], inflammatory skin disease, keratinocytes, TRPA1 ion channel

1 | INTRODUCTION

Allergic contact dermatitis (ACD) is a frequent inflammatory skin disease and a major cause of occupational morbidity, affecting up to 20% of the population worldwide (Brites et al., 2020). It is a prototypical T-cell-mediated delayed-type hypersensitivity reaction, typically presenting with erythema, oedema, vesiculation and intense pruritus after skin exposure to reactive chemicals known as contact sensitisers. Although ACD is classically considered an adaptive immune disorder, increasing evidence highlights the importance of innate immune activation and keratinocyte stress responses in disease initiation (Brites et al., 2020; Moyle et al., 2019).

The disease develops through a biphasic immune mechanism consisting of a sensitisation and an elicitation phase. During sensitisation, small reactive molecules penetrate the skin and bind covalently to proteins, forming hapten-protein complexes. This process activates keratinocytes, which release proinflammatory cytokines including **IL-1α**, **IL-1β**, **TNF-α**, **IL-8 (CXCL8)**, **IL-18** and **GM-CSF**, thereby amplifying innate immune responses (Gaspari, 1997; Yamaguchi et al., 2023). Antigen-presenting cells such as Langerhans cells and dermal dendritic cells internalise these haptenated proteins and migrate to draining lymph nodes, where they prime naïve T-cells. Antigen-specific T helper subsets (Th1, Th2 and Th17) and regulatory T-cells are subsequently generated and circulate as effector and memory populations (Brys et al., 2020). Upon re-exposure to the allergen, in the elicitation phase, hapten-specific memory T-cells rapidly recognise the antigen and release cytokines including **IFN-γ**, **IL-2** and IL-17, driving infiltration of inflammatory cells into the skin and producing the clinical features of ACD (Dhingra et al., 2014; Yamaguchi et al., 2023). Recent studies highlight the hapten-specific nature of these responses; nickel primarily induces Th1 and Th17-mediated pathways, whereas rubber and fragrance allergens preferentially trigger Th2 responses (Dhingra et al., 2014).

Contact sensitisers vary in potency and chemical reactivity. Strong sensitisers such as 2,4-dinitrochlorobenzene (DNCB), 2,4-dinitrofluorobenzene (DNFB), oxazolone and formaldehyde are widely used in experimental models of ACD (Ma et al., 2023; Moilanen et al., 2012). In addition to adaptive immune activation, contact sensitisers also trigger innate immune pathways by directly inducing stress responses in keratinocytes, leading to the release of alarmins and cytokines that amplify cutaneous inflammation (Das et al., 2022). More recently, epithelial danger sensing has been recognised as a critical checkpoint that determines the amplitude of skin inflammation. Keratinocytes integrate chemical stress signals and alarmin release to shape downstream immunity (Mendoza et al., 2025). This underscores the importance of investigating epithelial channels such as **Transient Receptor Potential Ankyrin 1 (TRPA1)** as frontline sensors in ACD.

TRPA1 is a non-selective cation channel best characterised in sensory neurons, where it mediates responses to reactive irritants, contributing to neurogenic inflammation and itch in ACD (Liu et al., 2013). This has led to the prevailing view that neuronal TRPA1 is the major driver of allergen-induced inflammation. However, TRPA1 expression has also been reported in non-neuronal skin cells, including keratinocytes, melanocytes and fibroblasts (Atoyan et al., 2009; Landini et al., 2022). The functional significance and precise epidermal localisation of keratinocyte TRPA1 have remained incompletely defined, in part due to limitations of immunohistochemical approaches and the need for more reliable localisation methods (Atoyan et al., 2009).

Accumulating evidence indicates that TRPA1 functions as a polymodal danger sensor in the skin, responding to electrophilic chemicals, oxidative stress and inflammatory mediators that are highly relevant to ACD (Andersson et al., 2008; Bautista et al., 2013). TRPA1

What is already known?

- Neuronal TRPA1 contributes to allergic contact dermatitis.
- Strong contact sensitisers activate TRPA1 channels.

What does this study add?

- Keratinocyte TRPA1 drives allergen induced cytotoxicity and IL-1α release.
- Allergen binding mode predicts TRPA1 activation strength.

What is the clinical significance?

- TRPA1 antagonism protects keratinocytes and may reduce allergic contact dermatitis (ACD) severity.

activation induces Ca^{2+} influx-dependent stress responses, mitochondrial dysfunction and reactive oxygen species generation, thereby amplifying inflammatory signalling cascades (Andersson et al., 2008; Trevisani et al., 2007). While these mechanisms have been extensively characterised in sensory neurons, where TRPA1 drives neurogenic inflammation, vasodilation and pruritus (Feng et al., 2017; Liu et al., 2013), keratinocytes are directly exposed to contact sensitisers and are therefore ideally positioned to engage TRPA1-mediated epithelial danger sensing. However, direct functional evidence for keratinocyte TRPA1 in allergen-induced cytotoxicity and inflammatory signalling in ACD remains limited, in part due to the predominance of neuron-centric models (Atoyan et al., 2009; Liu et al., 2013).

We therefore hypothesised that TRPA1 expressed in keratinocytes is a key driver of allergen-induced cytotoxicity and inflammatory signalling in ACD. Specifically, we asked:- (1) Do strong contact sensitisers directly activate TRPA1? (2) Does keratinocyte TRPA1 contribute functionally to the patho-mechanism of ACD? (3) do allergen-TRPA1 binding modes correlate with their biological potency? To address these questions, we used a multimodal approach combining *in vitro* assays using primary keratinocytes and human (h) TRPA1-transfected CHO cells, RNAscope localisation of TRPA1 in human and murine skin, *in vivo* oxazolone-induced hypersensitivity models and *in silico* docking studies.

2 | METHODS

2.1 | Animals

Naïve male wild-type (WT; *Trpa1*$^{+/+}$) and *Trpa1* knockout (KO; *Trpa1*$^{-/-}$) mice on a C57BL/6J genetic background (8–10 weeks of age, body weight 20–25 g) were used in this study. Animals had no prior experimental manipulation before inclusion. Mice were group-housed (four to five animals per cage) in individually ventilated cages (365 mm x 207 mm x 104 mm) under standard laboratory conditions, with a 12-h light/dark cycle, controlled ambient temperature (24°C–25°C) and relative humidity of 40%–60%. Environmental enrichment was provided, and animals had *ad libitum* access to chow and water. Only male mice were used to minimise variability associated with oestrous cycle-dependent hormonal fluctuations, which are known to influence cutaneous immune and inflammatory responses in contact hypersensitivity models (Gilliver et al., 2007; Voskuhl, 2011). Male mice on a C57BL/6J background were also used for RNAscope *in situ* hybridisation experiments. WT and *Trpa1* KO mice ($n = 18$) were studied in the oxazolone-induced ACD model.

The *Trpa1* KO mouse line was originally generated as described previously (Bautista et al., 2006). The animals were bred and kept in the Laboratory Animal House of the Department of Pharmacology and Pharmacotherapy of the University of Pécs.

All procedures at the University of Pécs were carried out according to the *1998/XXVIII* Act of the Hungarian Parliament on Animal Protection and Consideration Decree of Scientific Procedures of Animal Experiments (243/1988). All experiments were approved by the Ethics Committee on Animal Research of the University of Pécs, according to the Ethical Codex of Animal Experiments, and the license was given (license number: BA02/2000-15/2023). Animal studies were also reported in compliance with the ARRIVE guidelines (Percie du Sert et al., 2020) and with the recommendations made by the British Journal of Pharmacology (Lilley et al., 2020).

All terminal procedures were performed under deep anaesthesia and animals were killed as described in the relevant experimental sections.

2.2 | Preparation of reagents for the *in vivo* study

A 2% oxazolone solution (Sigma-Aldrich, St Louis, MO, USA) was freshly prepared before each experiment. The concentration of oxazolone (2%) was selected based on previous studies demonstrating robust and reproducible induction of ACD in mice (Liu et al., 2013). The selective TRPA1 antagonist **HC-030031(HC030031)** (Tocris Bioscience, Bristol, UK) was administered at a dose of 200 $mg \cdot kg^{-1}$, which has been shown to effectively inhibit TRPA1-mediated inflammatory and vascular responses *in vivo*, including in models of ACD (Moilanen et al., 2012; Pozsgai et al., 2017).

2.3 | Induction of a CHS response to oxazolone

C57BL/6J WT and *Trpa1* KO mice were anesthetised by intraperitoneal (i.p.) administration of medetomidine (1 $mg \cdot ml^{-1}$; Orion Pharma, Finland) and ketamine (75 $mg \cdot kg^{-1}$; Richter Gedeon, Hungary). During anaesthesia, mice maintained spontaneous breathing. Body temperature was maintained using thermostatically controlled heating pads and animals were continuously monitored throughout the procedure. Mice were sensitised by topical application of 2% oxazolone (Sigma-Aldrich, St Louis, MO, USA) in 96% ethanol on the shaved abdomen (50 µl). Five days later, mice were challenged by the topical application of 15 µl of 2% oxazolone on each side of one ear. In contrast, 15 µl of the vehicle (96% ethanol) was applied to the contralateral ear. Experiments were performed at 0, 24 and 48 h after challenge. Following anaesthesia mice were maintained on a heating pad and monitored continuously until full recovery from anaesthesia, after which they were returned to their home cages. No antibiotics or additional analgesics were administered, as the procedures were minimally invasive and conducted in accordance with institutional regulations and ARRIVE 2.0 guidelines. At the experimental endpoint, animals were euthanised under deep anaesthesia in accordance with institutional regulations and ARRIVE 2.0 guidelines. These time points were selected to capture baseline conditions (0 h), the peak of ear oedema and vascular responses (24 h) and the subsequent inflammatory phase (48 h), in accordance with the established temporal kinetics of the oxazolone-induced contact hypersensitivity model (Bánvölgyi et al., 2005).

2.4 | TRPA1 antagonist treatment for the *in vivo* study

In the relevant groups, HC-030031 200 mg·kg^{-1} was subcutaneously (s.c.) administered once daily, 2 h before each oxazolone treatment throughout the experiment. The route, dose and timing of administration were selected based on established *in vivo* protocols demonstrating effective TRPA1 inhibition throughout the experimental setup.

2.5 | Measurement of ear thickness change in vehicle/oxazolone-treated ears

Ear thickness was measured with an engineer's micrometre (Moore and Wright, Sheffield, England) with 0.1-mm accuracy, before oxazolone treatment at different time points (0, 24 and 48 h). All measurements were performed under anaesthesia; therefore, no physical restraint was required. Data were expressed as a percent increase in ear thickness compared with Day 0 baseline initial values.

2.6 | Measurement of blood perfusion changes in vehicle/oxazolone-treated ears

Ear's blood flow was measured by Laser Speckle Contrast Analysis (LASCA) laser Doppler (Perimed, Sweden) (Banki et al., 2014; Pozsgai et al., 2012) method before daily application of oxazolone. Measurements were displayed as arbitrary perfusion/flux units. Regions of interest (ROI) were selected according to the treated areas on the ear skin and mean perfusion was generated by PimSoft software (Perimed, Sweden). All measurments were performed under anaesthesia; therefore, no physical restraint was required. Data were expressed as a percentage of blood perfusion change compared to the Day 0 values.

2.7 | Assessment of histological changes in the ears caused by vehicle/oxazolone treatment

Ear samples were formaldehyde-fixed (6%) and embedded in paraffin; 5-μm sections were cut and stained with haematoxylin and eosin to assess epidermal-dermal thickness and to quantify Munro's microabscesses. Morphological changes were evaluated using 200X magnification. The thickness of epidermal and dermal layers was measured with CellSens software (Version 3.1).

2.8 | Preparation of reagents for the *in vitro* study

2,4-dinitrofluorobenzene (DNFB) (Sigma-Aldrich, St Louis, MO, USA), 2,4-dinitrochlorobenzene (DNCB) (Sigma-Aldrich, St Louis, MO, USA), 6% formaldehyde (Molar chemical kft, Halásztelek, Hungary) and oxazolone (Sigma-Aldrich, St Louis, MO, USA) were prepared as stock solutions (2, 2, 10 and 10 mM, respectively).

The 10–300 μM of DNCB, 1–30 μM of DNFB, 300–1000 μM of formaldehyde and 25–200 μM of oxazolone were prepared from the stock solutions diluted using extracellular solution (ECS), which was prepared in-house by the Department of Pharmacology and Pharmacotherapy, University of Pécs (Hungary), according to standard laboratory protocols.

A 100 mM stock solution of **mustard oil (allyl isothiocyanate)** (Sigma-Aldrich, St Louis, MO, USA) in dimethyl sulfoxide (DMSO) (Sigma-Aldrich Co., Steinheim, Germany), and a 100 mM stock solution of HC-030031 (Tocris Bioscience, Bristol, United Kingdom) in DMSO were prepared and subsequently diluted in extracellular solution to final concentrations of 100 μM for MO and 10 μM or 20 μM for HC-030031, before each experiment. These compounds were used to treat the cells for intracellular calcium measurement, ATP viability assay and cytokine release analysis.

The concentration ranges of contact sensitisers used in the *in vitro* experiments were selected based on previous studies demonstrating TRPA1 activation, keratinocyte toxicity or contact hypersensitivity-related cellular responses, while avoiding non-specific solvent toxicity. DNCB and DNFB were applied in the micromolar range previously shown to induce keratinocyte stress responses and TRPA1 activation in cell-based assays (Lian et al., 2022; Mäki-Opas et al., 2023). Formaldehyde concentrations were chosen based on established *in vitro* toxicity and inflammatory signalling studies in skin-relevant cell types (Ma et al., 2023). For oxazolone, no established *in vitro* concentration ranges were identified in the literature for direct cellular calcium signalling assays. Therefore, oxazolone concentrations were determined empirically in our laboratory by performing preliminary dose–response experiments to identify the lowest concentration capable of reliably evoking TRPA1-dependent intracellular Ca^{2+} influx. The TRPA1 antagonist HC-030031 (10 or 20 μM) and the TRPA1 agonist mustard oil (100 μM) were used at concentrations widely employed to achieve effective and selective TRPA1 modulation *in vitro* (Macpherson et al., 2007; Pozsgai et al., 2017).

2.9 | Cell lines

Naïve Chinese hamster ovarian (CHO) cells (Sigma-Aldrich, RRID: CVCL_0214) and overexpressing human TRPA1 channel (TRPA1^{+}) CHO cells were given to us by our colleague Dr. Zoltán Sándor (Pozsgai et al., 2017).

Primary keratinocytes were isolated from WT and *Trpa1* KO mouse strains according to a previously described protocol (Li et al., 2017), involving enzymatic separation of the epidermis followed by dissociation and culture of keratinocytes.

CHO cells were cultured in Dulbecco's Modified Eagle's Medium (DMEM, Thermo Fisher Scientific, Waltham, MA, USA) supplemented with 4-mmol L-glutamine, 10% fetal bovine serum (FBS) and 1 × penicillin/streptomycin (Thermo Fisher Scientific), and non-essential amino acids (Sigma-Aldrich, St Louis, MO, USA).

Primary keratinocytes were cultured in CNT-07 epithelial cell culture media (CELLnTEC Advanced Cell Systems AG, Bern, Switzerland) supplemented with 10% fetal bovine serum, 1 × penicillin/streptomycin (Thermo Fisher Scientific) and 1.25-μg·ml^{-1} Fungizone.

All cells were maintained at 37°C within a 5% CO_2 incubator.

2.10 | Measurement of cellular calcium influx

The naïve CHO cell, TRPA1^{+} CHO, and WT primary keratinocytes were investigated for the activation of TRPA1 using all four allergens at different concentrations.

The cells were seeded in a 96 well μ-plate at 10,000 cells per well and incubated at 37°C with 5% CO_2 overnight before the experiment.

The next day, the culture medium was removed. The cells were loaded with Fura-2 (Invitrogen, USA) and incubated for 45 min at 37°C with 5% CO_2. Subsequently, the cells were washed with extracellular solution and incubated for 10 min at 37°C with 5% CO_2.

Intracellular Ca^{2+} measurements were performed using a Clariostar plate reader, which automatically injected defined concentrations of DNCB, DNFB, oxazolone or formaldehyde into the designated wells. Each well was assigned to a single experimental condition. In antagonist-treated groups, cells were pretreated with the TRPA1 antagonist HC-030031 for 30 min prior to baseline recording and subsequent allergen application. Baseline fluorescence was recorded for 10 s, after which the known TRPA1 agonist mustard oil (100 μM) was applied as a positive control, extracellular solution as a negative control, or the indicated allergen concentrations, and fluorescence was recorded for an additional 110 s. Responses were normalised to mustard oil -induced TRPA1 activation. All allergen concentrations, antagonist conditions and controls were tested in independent wells, without reuse.

2.11 | ATP luminescent cell viability assay

Naïve and TRPA1^{+} CHO cells, as well as WT and *Trpa1* KO primary keratinocytes, were seeded into opaque 96-well plates at a density of 10,000 cells per well and incubated overnight at 37°C with 5% CO_2. On the following day, the culture medium was removed and, where indicated, cells were pretreated with 20-μM HC-030031 for 30 min prior to the addition of the allergens at the designated concentrations. After allergen treatment, CellTiter-Glo® reagent (Promega, Madison, WI, USA) was added directly to all wells. The plates were placed on a shaker (with moderate speed) at room temperature for 5 min, followed by an additional 15-min incubation at room temperature. An ATP-based luminometric measurement of the metabolically active cells in the culture were determined by an EnSpire® Multimode Plate Reader (Waltham, MA, USA) as relative light units (RLUs). Viability was calculated as follows:-

$$\text{viability}\,(\%) = \text{RLU of experiment well}/\text{RLU of control well} \times 100.$$

2.12 | Preparation of human skin samples for RNAscope *in situ* hybridisation

The 5-mm full-thick skin biopsies were obtained from the gluteal area of healthy volunteers (n = 3) at the Department of Dermatology, Venereology and Oncodermatology, University of Pécs. The study protocol was approved by the Regional Research Ethics Committee of the University of Pécs, with the approval number of 7392–PTE 2018, adhering to Helsinki guidelines. Written informed consent was obtained from all subjects. The tissue samples were post-fixed in 4% paraformaldehyde solution for 72 h at 4°C, then embedded in paraffin. A microtome (Thermo Fisher Scientific) was used to cut 5-μm sections, which were then mounted on Superfrost Ultra Plus slides (Thermo Fisher Scientific, Walthan, MA, USA).

2.13 | Preparation of animal skin samples for RNAscope *in situ* hybridisation

Naïve C57BL/6J mice (n = 4) were deeply anaesthetised with urethane (2.4 g·kg^{-1}, intraperitoneally) and subsequently killed by transcardial perfusion with 30 ml of an ice-cold 0.1-M phosphate-buffered saline (PBS) (pH 7.4), followed by 150 ml of 4% paraformaldehyde (PFA) solution in Millonig buffer (pH 7.4). Shaved skin tissue samples were collected after the perfusion and post-fixed in the same fixative solution for 72 h at 4°C. Then, using a microtome, paraffin-embedded sections were prepared for the RNAscope study, as described for the human samples.

2.14 | RNAscope *in situ* hybridisation combined with immunostaining

All the immuno-related procedures used comply with the recommendations made by the *British Journal of Pharmacology* (Alexander et al., 2018).

RNAscope *in situ* hybridisation was performed according to Wang et al. (Wang et al., 2012). Sections were incubated for 60 min at 60°C. According to the user manual of the RNAscope Multiplex Fluorescent Reagent Kit v2 (ACD, Hayward, CA, USA), the steps of the RNAscope protocol were performed, including pretreatment, probe hybridisation, signal amplification and channel development. To detect TRPA1 mRNA in the skin, mouse *Trpa1* (ACD, Cat. No.: 400211) and a human *TRPA1* (ACD, Cat. No.: 837411) probes were applied, visualised by cyanine 3 (Cy3) dye (1:750). Mouse (ACD; Cat. No.: 320881) and human (ACD; Cat. No.: 320861) 3-plex positive and negative (ACD; Cat. No.: 320871) control probes were tested on skin samples as a technical control. The 3-plex technical positive control probes gave a well-detectable signal, while the negative control probes did not give any recognisable fluorescence in the preparations.

After the RNAscope *in situ* hybridisation protocol, immunofluorescence labelling was performed with the rabbit cytokeratin

14 (CK14) primary antibody (1:500; Abcam, Cat# ab181595, RRID: AB_2687525) for 24 h at 24°C. After washing with PBS for 2 × 15 min, samples were incubated with Alexa488-conjugated donkey anti-rabbit secondary antibody (1:500; Jackson ImmunoResearch, Cat# 711-545-152, RRID: AB_2313584) for 3 h. After washing with PBS for 2 × 15 min, sections were treated with 4′,**6-diamidino-2-phenylindole (DAPI)** to visualise the nuclei. After PBS washing, slides were covered with ProLong Gold Antifade (Thermo Fisher Scientific, Waltham, MA, USA; Cat. No. P10144) medium and stored at −20°C until digitalisation.

2.15 | Microscopy and digital imaging

Microscopic preparations were analysed using an Olympus FluoView 1,000 confocal microscope (Olympus, Hamburg, Germany). In order to reliably detect and identify quantifiable fluorescent signal, as well as prevent false positive signals caused by slightly overlapping emission spectra, digital images were obtained by sequential scanning in analogue mode for the appropriate fluorophores. For scanning, the confocal aperture was set to 80 µm, with a 40X/60X objective and 1024 × 1024-pixel resolution. The digital scans had an optical thickness of 3.5 µm. By applying the built-in parameters of the FluoView software (FV10-ASW; Version 0102, Olympus, Hamburg, Germany), the excitation and emission spectra for the appropriate fluorophores were chosen. Alexa488 was excited at 488 nm, Cy3 at 550 nm and DAPI at 405 nm.

Each section was scanned at three channels for their respective wavelength. Digital scan imaging of these channels showed the same area and were automatically superimposed and merged.

2.16 | Luminex assay

2.16.1 | Sample preparation

Primary keratinocytes were cultured in six-well plates (1×10^6 cells per well). For each experimental group, three independent cultures were prepared and treated according to the designated conditions for the specified durations. Following treatment of primary keratinocyte WT and KO cells with allergens for 12 h, culture supernatants were collected. Cells were subsequently harvested and centrifuged at 10,600 × g for 5 min to isolate intracellular fractions containing cytokines. All samples were stored at −20°C until further analysis.

2.16.2 | Immunoassay procedure

MILLIPLEX® high-sensitivity Mouse Antibody Magnetic Bead Panel kits were obtained from Millipore Sigma (Burlington, MA, USA). These panels utilise specifically designed magnetic beads to detect antibodies, including IL-1α, IL-1β, IL-6, **IL-4**, keratinocyte chemoattractant (KC) and **MCP-1 (CCL2)**. The immunoassay was performed according to the manufacturer's instructions. Briefly, supernatant samples were incubated with the magnetic beads in 96-well plates overnight at 4°C. The plates were then washed twice using Wash Buffer. Detection antibody solution was added to each well, followed by a 60-min incubation at room temperature. Subsequently, Streptavidin-Phycoerythrin was added, and the plates were incubated for an additional 30 minutes. After two more washes with Wash Buffer, Sheath Fluid PLUS was added to each well. The plates were analysed using the Luminex® MagPix platform, and median fluorescent intensity (MFI) data were generated and processed using xPONENT software for further analysis.

In silico *modelling*

Ligand preparation. DNFB, DNCB, oxazolone and formaldehyde were built in Maestro (Schrödinger, 2024), and a local steepest descent quick energy minimisation was performed in the Maestro graphical user interface. DNFB was also docked with the non-covalent mode of FITTED (Corbeil et al., 2007; Therrien et al., 2014), where built-in preparatory steps were used with default settings to prepare DNFB for docking.

Target preparation. Atomic coordinates of the human TRPA1 receptor in complex with a covalent agonist were obtained from the Protein Data Bank (PDB (Berman, 2000) with PDB code 6pqp (Suo et al., 2020). Only chain A was used from the homotetramer structure to reduce computational costs (Zsidó et al., 2021). Missing residues were rebuilt with SWISS-MODEL (Waterhouse et al., 2018), and energy minimised with GROMACS (Van Der Spoel et al., 2005), as described in (Zsidó et al., 2021). For docking with Glide (Friesner et al., 2004), a grid box was prepared in Maestro centred on the C621 amino acid, with 20-Å sides, and for covalent mode, C621 was selected as the covalent residue; for non-covalent mode, this was skipped. For FITTED, the built-in target preparatory steps were executed with default settings.

Docking. The non-covalent and covalent function of FITTED was used with default settings. No covalent warhead was detected for DNFB; therefore, only non-covalent binding modes (five) were printed out. In the case of covalent docking with Glide, the covalent docking of DNFB and DNCB were possible after specifying nucleophilic substitution as the covalent binding mechanism, and for formaldehyde, the nucleophilic addition to a double bond was selected as the reaction type. For oxazolone, no covalent reaction type was applicable. For FITTED, the original covalent agonist was kept in the structure to define the binding site, which was then automatically removed during docking. For Glide, the C621 amino acid was specified as a covalent residue in covalent mode. Flexibility around torsions was enabled for both programmes; otherwise, default settings were used. In Glide, Prime post-docking minimisation was also performed with default settings.

2.17 | Statistical analysis

This study was designed, conducted, analysed and reported in accordance with the recommendations set out in the *British Journal of*

Pharmacology (BJP) editorials and guidelines (Curtis et al., 2025). Results are presented as mean ± SEM. Statistical analyses were performed using GraphPad Prism version 10.5 for iOS (GraphPad Software, San Diego, CA, USA). Calcium influx measurements were normalised to mustard oil induced activity and analysed using one-way ANOVA. ATP-based luminescent cell viability assay data were analysed using one-way ANOVA followed by Šídák's multiple comparisons test. Post hoc tests were conducted only if the overall ANOVA achieved $P < 0.05$. Luminex measurements were performed using $n = 3$ independent biological replicates, each analysed in technical duplicate. Due to the limited number of biological replicates and the exploratory nature of the multiplex screening, no formal statistical testing was applied to these data and results are presented descriptively. For the *in vitro* experiments, independent biological experiments were performed on separate days using independently prepared cell cultures. For each condition, multiple independently prepared biological samples (independent cultures) were analysed and each sample was measured in technical replicates. Technical replicates were averaged to yield a single value per biological sample and statistical analyses were performed using these biological sample values; n denotes the number of independent biological samples per condition. For multiplex cytokine analysis, a limited number of independent biological replicates were analysed (each measured in technical duplicate), consistent with exploratory, hypothesis-generating Luminex screening and interpreted in conjunction with the robust *in vivo* findings. For *in vivo* experiments, n represents the number of individual animals. Where applicable, procedures involving immunohistochemistry and image-based analyses were performed in accordance with the relevant *BJP* recommendations for rigour and reproducibility. Randomisation and blinding were not applied due to the nature of the experimental design; however, all procedures were performed using standardised protocols and consistent experimental conditions to minimise potential bias.

2.18 | Materials

All chemicals, reagents, materials and resources used are described in detail in the methods section, including the reagent preparation subsections for both *in vitro* and *in vivo* experiments. Key compounds include DNCB, DNFB, oxazolone, and MO (all from Sigma-Aldrich, St. Louis, MO, USA) formaldehyde (Molar Chemical Kft, Hungary) and the selective TRPA1 antagonist HC-030031 (Tocris Bioscience, Bristol, UK). A comprehensive list of all the materials including suppliers, catalogue numbers and Research Resource Identifiers (RRID), is provided in Table S2.

2.19 | Nomenclature of targets and ligands

Key protein targets and ligands in this article are hyperlinked to corresponding entries in the IUPHAR/BPS Guide to PHARMACOLOGY http://www.guidetopharmacology.org and are permanently archived in the Concise Guide to PHARMACOLOGY 2025/2026 (Alexander, Striessnig, et al., 2025; Alexander, Fabbro, et al., 2025).

3 | RESULTS

3.1 | TRPA1 is essential for oxazolone-induced allergic contact dermatitis (ACD)

We first evaluated the role of TRPA1 in our oxazolone-induced acute model of ACD. WT mice developed robust oedema (ear swelling) following oxazolone challenge, indicative of inflammatory activation, whereas *Trpa1* KO mice exhibited a markedly reduced oedema response. Similarly, pharmacological inhibition of TRPA1 with HC-030031 significantly suppressed oedema formation in WT mice at both 24 and 48 h post-challenge (Figure 1a,b). Laser speckle imaging showed that blood perfusion increased in WT mice at 24 h but was not sustained at 48 h, and this vascular response was significantly attenuated in *Trpa1* KO and HC-pretreated mice (Figures 1b and S1).

Histopathological analysis further demonstrated clear oedema, inflammatory infiltration, and Munro's microabscess formation in WT mice, while they were significantly reduced in *Trpa1* KO and HC-030031 pretreated WT animals (Figure 1c–e).

Haematoxylin-eosin sections also showed increased dermal cellular infiltration after oxazolone challenge, which was reduced in *Trpa1* KO and HC-030031 pretreated WT mice. While the present study did not include immune cell phenotyping, the oxazolone contact hypersensitivity model is well known to involve an early neutrophil rich infiltrate followed by accumulation of T-cells and other leukocyte populations during the elicitation phase. Notably, the presence of Munro's microabscesses in our sections is consistent with focal collections of neutrophils within the epidermis/stratum corneum (Honda et al., 2013; King, 1979; Lv et al., 2015; Tuckermann et al., 2007).

Although minor qualitative differences were observed in representative haematoxylin-eosin stained sections of vehicle-treated WT and *Trpa1* KO ears, quantitative morphometric analysis revealed no statistically significant differences in epidermal-dermal thickness between genotypes under baseline conditions. These subtle visual variations likely reflect normal inter-individual variability and sectioning orientation rather than genotype-dependent structural alterations. Importantly, genetic deletion of Trpa1 did not alter epidermal architecture or inflammatory cell presence in vehicle-treated ears, indicating that TRPA1 does not affect healthy skin morphology under baseline conditions.

3.2 | Strong contact sensitisers activate TRPA1

To assess TRPA1 activation by allergens, we performed calcium fluorescence imaging (Fura-2 AM) in naïve and TRPA1^{+} CHO cells. DNCB (10–300 μM), DNFB (1–30 μM), formaldehyde (30–1000 μM) and oxazolone (25–200 μM) produced concentration-dependent increases in intracellular Ca^{2+} levels, comparable to the TRPA1 agonist mustard

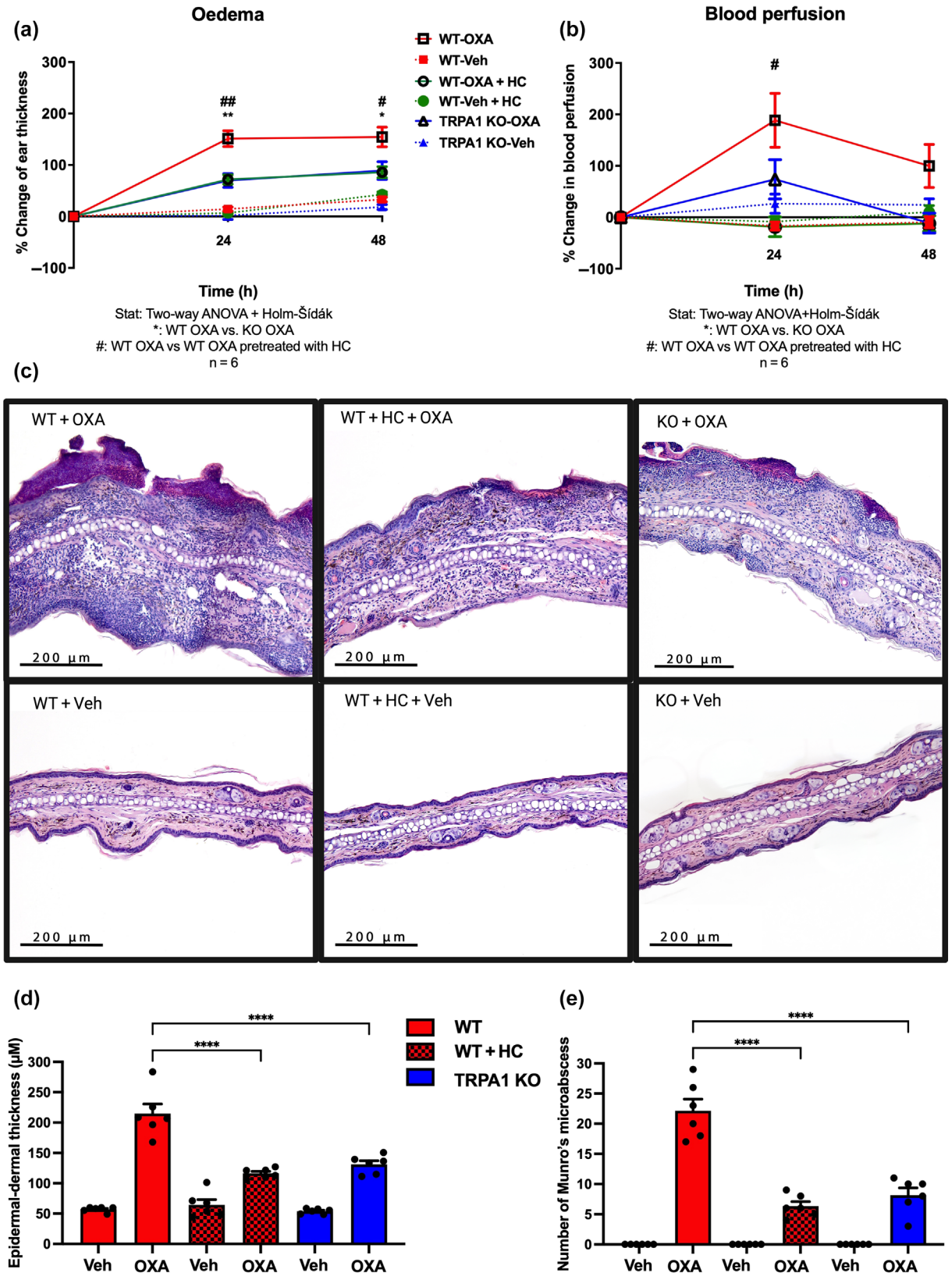

FIGURE 1 Legend on next page.

oil (100 μM). No calcium influx was observed in naïve CHO cells or TRPA1$^+$ cells pretreated with HC-030031, confirming TRPA1 specificity (Figure 2).

3.3 | Strong contact sensitisers induce cytotoxicity via TRPA1

To further assess the consequences of TRPA1 activation, we examined cell viability in TRPA1$^+$ and naïve CHO cells. ATP-based luminescent viability assays demonstrated that exposure to DNCB, DNFB, formaldehyde and oxazolone led to a concentration-dependent reduction in viability exclusively in TRPA1$^+$ CHO cells, whereas naïve cells remained unaffected. Importantly, pretreatment with the selective TRPA1 antagonist HC-030031 significantly attenuated cytotoxicity and rescued TRPA1$^+$ cells from allergen-induced death (Figure 3).

3.4 | Human and mouse keratinocytes express TRPA1

Next, to examine TRPA1 expression in keratinocytes, skin samples from healthy mice and humans were analysed using RNAscope *in situ* hybridisation. In mouse skin, where the epidermis consists of a single keratinocyte layer, TRPA1 transcripts (red) were clearly detected and co-localised with the basal marker cytokeratin 14 (CK14; green). In human skin, TRPA1 expression was likewise concentrated in basal keratinocytes, while only minimal signal was observed in suprabasal layers, indicating that TRPA1 expression is largely restricted to the basal compartment of the epidermis (Figure 4). The present study focused on TRPA1 expression in healthy mouse and human skin to establish baseline keratinocyte localisation; whether TRPA1 expression is dynamically regulated in allergen exposed or lesional ACD skin remains an important question for future investigation.

3.5 | Strong contact sensitisers induce TRPA1-dependent cytotoxicity in keratinocytes

Next, to assess TRPA1 activation in a physiologically relevant setting, primary keratinocytes isolated from WT and *Trpa1* KO mice were exposed to contact allergens. WT keratinocytes displayed concentration-dependent cytotoxicity, whereas *Trpa1* KO keratinocytes maintained viability under identical conditions. Importantly, pretreatment of WT keratinocytes with the selective TRPA1 antagonist HC-030031 significantly reduced cytotoxicity, confirming TRPA1 dependence and identifying keratinocyte TRPA1 as a key mediator of allergen-induced cell death (Figure 5). Consistent with this, HC-030031 provided protection against the cytotoxic effects of all tested allergens (DNCB, DNFB, formaldehyde and oxazolone), highlighting TRPA1 antagonism as a promising therapeutic approach to limit keratinocyte damage in ACD.

3.6 | TRPA1-dependent IL-1α release from keratinocytes

To assess whether allergen-induced keratinocyte cytotoxicity was accompanied by cytokine release, we quantified IL-1α, IL-1β, IFN-γ, IL-4, keratinocyte chemoattractant (KC) and MCP-1 levels using a Luminex multiplex assay. Unstimulated (extracellular solution [ECS]-treated) keratinocytes from WT and *Trpa1* KO mice exhibited comparable baseline cytokine levels (see Figure S4), confirming that the observed changes in cytokine release were specifically induced by allergen exposure rather than reflecting intrinsic genotype-dependent differences. Among the measured cytokines, only IL-1α exhibited a consistent TRPA1-dependent response to allergen exposure. WT keratinocytes displayed higher IL-1α levels compared to *Trpa1* KO keratinocytes, and pretreatment with HC-030031 reduced IL-1α levels in WT keratinocytes (Figure 6). In contrast, other cytokines remained at low or biologically insignificant levels and did not exhibit a consistent TRPA1-dependent response pattern under these conditions. The notable exception was MCP-1, which was produced at comparable levels across WT, *Trpa1* KO and HC-030031-pretreated WT keratinocytes, indicating TRPA1-independent regulation. This pattern contrasts with the selective induction of IL-1α and identifies IL-1α as the primary TRPA1-dependent mediator of keratinocyte activation following allergen challenge. The preservation of MCP-1 production across genotypes and treatment conditions is consistent with basal chemokine release by keratinocytes and suggests the involvement of alternative signalling pathways distinct from TRPA1. Because multiplex cytokine measurements were performed with a limited number of biological replicates (n = 3), these data should be interpreted as exploratory and hypothesis-generating.

FIGURE 1 Pathological analysis of cutaneous inflammation in wild-type (WT), WT pretreated with HC-030031 (HC) and Transient receptor potential ankyrin 1 (*Trpa1*) knockout (KO) mice in acute oxazolone (OXA)-induced dermatitis on the ear. (a) Increase in ear thickness of WT mice, WT pretreated with HC and *Trpa1* KO mice, treated with vehicle or OXA (n = 6 mice per group). WT OXA group versus *Trpa1* KO OXA group ($^*P < 0.0332$; $^{**}P < 0.0021$), WT OXA versus WT OXA pretreated with HC ($^{\#}P < 0.0332$; $^{\#\#}P < 0.0021$). (b) Percentage increase in ear blood flow of WT mice, WT pretreated with HC and *Trpa1* KO mice, treated with vehicle (Veh) or OXA (n = 6 mice/group). WT OXA versus WT OXA pretreated with HC ($^{\#}P < 0.0332$). (c) Haematoxylin and eosin stained sections of ears from WT mice, WT pretreated with HC and *Trpa1* KO mice, treated with vehicle or OXA. Scale bar = 200 μm. (d) Measurements of epidermal thickness of WT mice, WT pretreated with HC and *Trpa1* KO mice, treated with vehicle (ethanol, left) or OXA (right) (n = 6 mice per group; $^{****}P < 0.0001$). (e) Munro's microabscess counts in sections of the ears of WT mice, WT pretreated with HC and Trpa1 KO treated with vehicle.

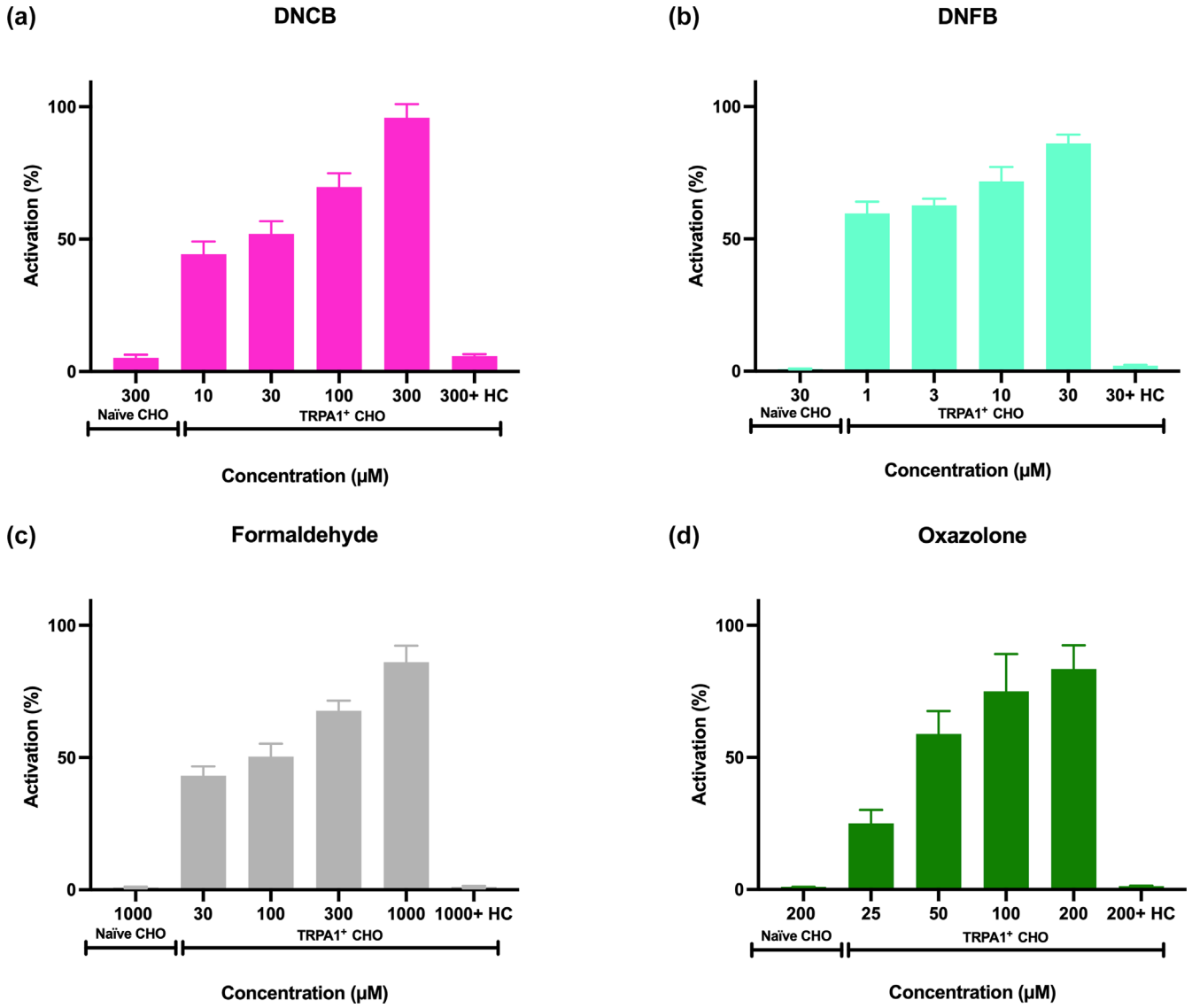

FIGURE 2 Calcium fluorescence assay in naïve and TRPA1^{+} CHO cells in response to the contact sensitisers 2, 4-dinitrochlorobenzene (DNCB) (a), 2,4-dinitrofluorobenzene (DNFB) (b), formaldehyde (c) and oxazolone (d). Data represent the normalised increase of intracellular Ca^{2+} levels relative to the TRPA1 agonist mustard oil (MO, 100 μM). Extracellular solution (ECS) served as the negative control, and HC-030031 (HC) was used as the TRPA1 antagonist. Data represent mean ± SEM of n = 6 biological replicates each in technical duplicate. Statistical analysis was performed using one-way analysis of variance (ANOVA).

3.7 | The binding mode of contact sensitisers partly explains their sensitising potency

Next, to provide mechanistic insight into TRPA1-allergen interactions (Figures 7 and 8; see Figures S5–S7), we performed *in silico* docking studies. DNFB covalently bound to cysteine C621 and interacted with A-loop residues I679 and Y680, stabilising the open conformation. This correlated with the most substantial Ca^{2+} influx and cytotoxicity *in vitro*. DNCB also bound covalently to C621 but did not engage the A-loop, consistent with weaker activity. Formaldehyde formed only limited interactions (T624 and T684), in line with its low potency. Oxazolone bound non-covalently but established multiple stabilising contacts (C621, C665, T624 and T684), explaining its intermediate activity compared with covalent agonists.

To assess species translatability, docking analyses were additionally performed using a mouse TRPA1 structure generated by AlphaFold. Comparable docking scores and binding modes were observed for mouse and human TRPA1 across all tested allergens, indicating conserved ligand–TRPA1 interactions (see supporting information supporting methods; Figure S8 and Table S1).

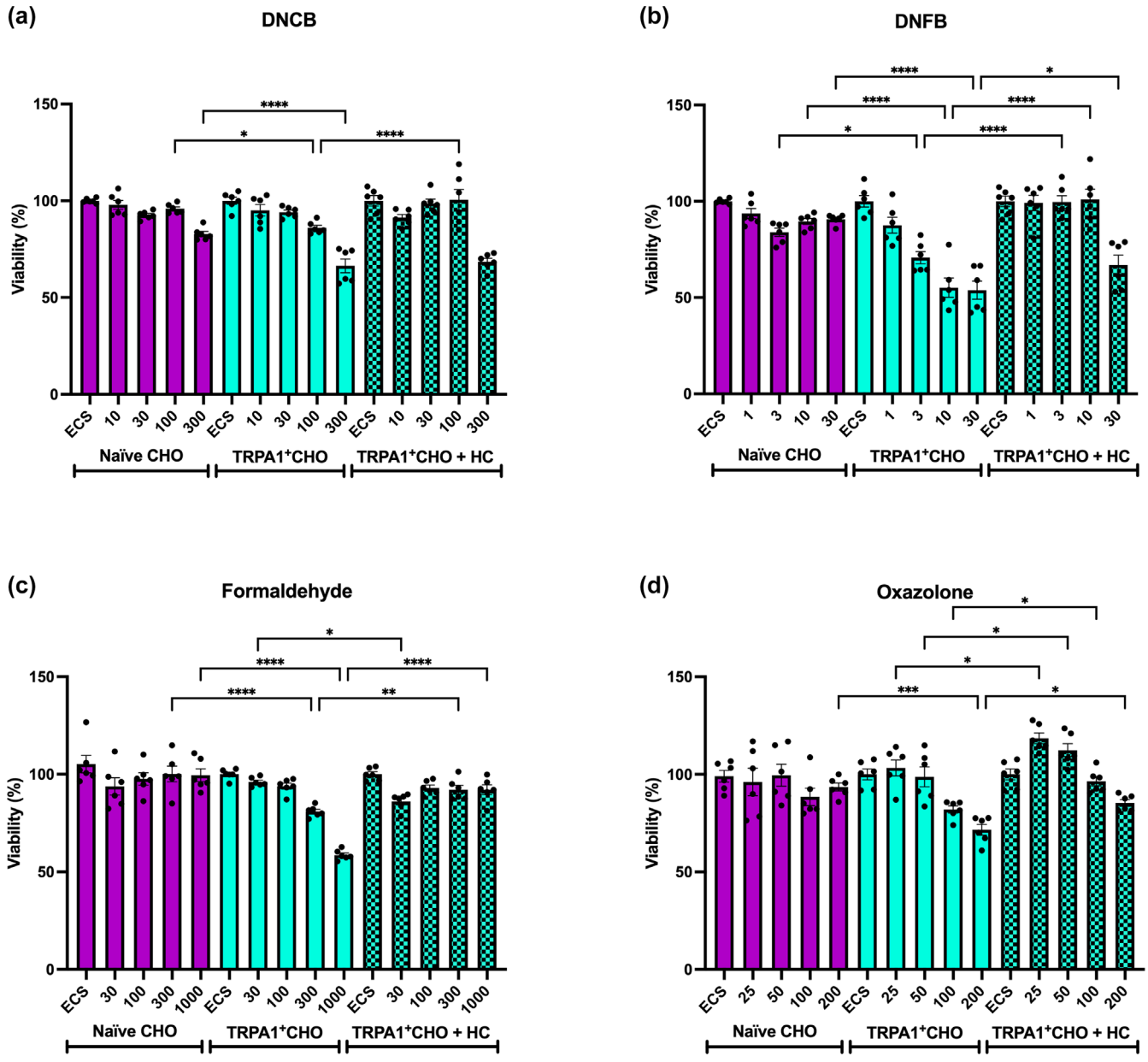

FIGURE 3 ATP luminescent cell viability assay in naïve and TRPA1$^+$ CHO cells following treatment with the contact sensitisers 2, 4-dinitrochlorobenzene (DNCB) (a), 2,4-dinitrofluorobenzene (DNFB) (b), formaldehyde (c) and oxazolone (d). Cell viability was assessed after exposure to increasing allergen concentrations to evaluate whether effects on viability were mediated through TRPA1. Purple bars represent naïve CHO cells, blue bars represent TRPA1$^+$ CHO cells and patterned bars represent TRPA1$^+$ CHO cells pretreated with the TRPA1 antagonist HC-030031. Allergen concentrations are shown in μM. ECS, extracellular solution, was used as a negative control. The TRPA1 agonist mustard oil (MO; 100 μM) was used as a positive control to validate assay specificity (see Figure S2). Data represent mean ± SEM of n = 6 biological replicates, each in technical triplicate. Statistical analysis was performed using one-way analysis of variance (ANOVA) with Šídák's post hoc test (*P < 0.0332, **P < 0.0021, ***P < 0.0002, ****P < 0.0001).

4 | DISCUSSION

In this study, we demonstrate that genetic deletion or pharmacological inhibition of TRPA1 markedly attenuates oxazolone-induced allergic contact dermatitis (ACD) *in vivo*, as evidenced by reduced ear oedema, vascular responses and histopathological alterations. Our findings highlight keratinocyte TRPA1 as a central sensor linking the chemistry of strong contact sensitisers to epidermal damage and inflammatory amplification in ACD. Traditionally, ACD has been viewed through the lens of adaptive immunity, in which hapten protein conjugates trigger dendritic cell activation and T-cell priming (Brys et al., 2020; Gaspari, 1997). Yet, before the adaptive response unfolds, the earliest events occur in keratinocytes, where reactive chemicals induce stress, cytotoxicity and cytokine release (Yamaguchi

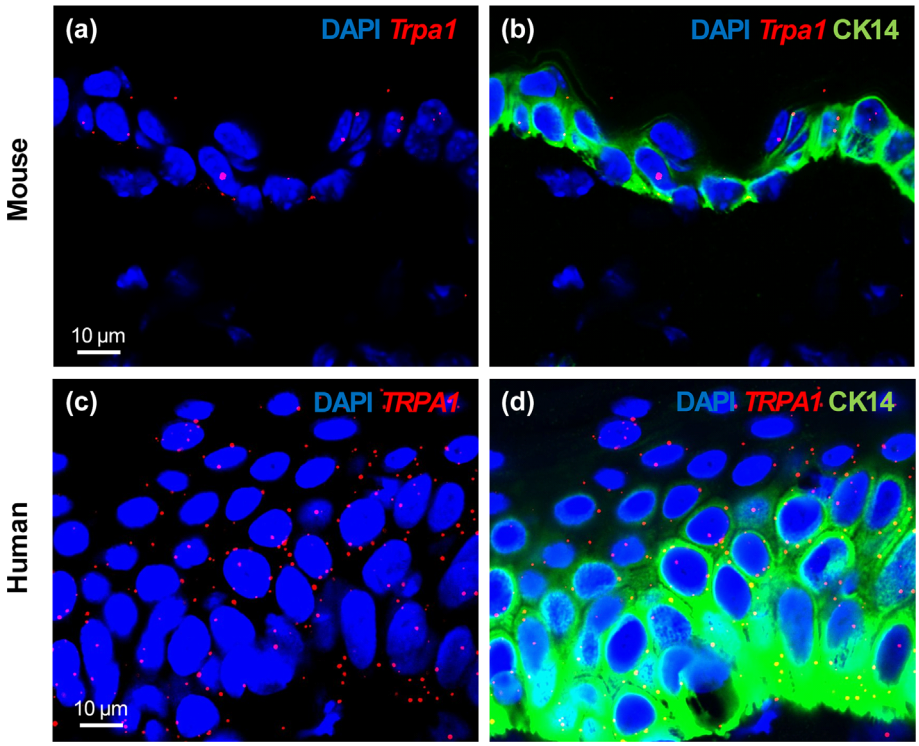

FIGURE 4 Transient receptor potential ankyrin 1 (Trpa1/TRPA1, red) mRNA transcripts and cytokeratin 14 (CK14, green) protein (keratinocyte marker) in mouse (a and b) and human (c and d) skin tissues with 4′,6-diamidino-2-phenylindole (DAPI, blue) nuclear staining. Images are representative of three independent experiments. Human skin samples were obtained from multiple donors and TRPA1 expression patterns were consistent across samples.

et al., 2023; Ye & Lai, 2025). Our work provides mechanistic evidence that TRPA1 integrates these initial danger signals, positioning keratinocyte TRPA1 upstream of immune amplification.

Histological analysis revealed prominent inflammatory cell infiltration following oxazolone challenge, which was markedly attenuated by genetic deletion or pharmacological inhibition of TRPA1. In the oxazolone-induced contact hypersensitivity model, leukocyte recruitment is well characterised and is dominated by an early neutrophil-rich infiltrate peaking around 24 h, followed by the accumulation of antigen-specific T-cells and other immune cell populations during the elicitation phase (Lv et al., 2015; Martinov et al., 2013). Consistent with this established framework, the presence of Munro's microabscesses in our sections is compatible with focal collections of polymorphonuclear leukocytes, predominantly neutrophils, within the epidermis and stratum corneum (King, 1979; Uribe-Herranz et al., 2013). While the present study did not aim to characterise immune cell subpopulations in detail, the reduction in inflammatory infiltrates supports a model in which keratinocyte TRPA1 activity contributes to the initiation and amplification of cutaneous inflammation.

At the molecular level, to explain these differential epithelial responses, our *in vitro* and *in silico* data indicate that the binding mode of contact sensitisers at TRPA1 critically influences the magnitude of Ca^{2+} influx and the downstream cytotoxic response. Electrophilic allergens such as DNFB and DNCB covalently modify cysteine residues (notably C621) and when stabilising the A-loop in its open conformation-produce robust TRPA1 activation (Macpherson et al., 2007; Suo et al., 2020). In contrast, oxazolone, though binding non-covalently, still establishes multiple stabilising interactions, explaining its intermediate potency. These structure–activity relationships mirror cryo-EM findings that covalent anchoring and loop stabilisation are central to agonist efficacy (Paulsen et al., 2015).

Docking analyses were performed using the human TRPA1 structure due to the availability of high-resolution cryo-EM data. Human and mouse TRPA1 share high sequence conservation within the electrophile-sensitive, cysteine-rich intracellular domain that mediates covalent agonist binding, suggesting that the identified binding modes are likely conserved across species. Nevertheless, future comparative modelling using mouse TRPA1 structures would further strengthen translational interpretation.

The agonist-induced open conformation of the binding site also increases the accessibility of reactive cysteines, making them more susceptible to oxidative modification by ROS. This suggests a mechanistic link between covalent allergen binding and redox amplification. In turn, allergens that stabilise the open state not only drive strong initial activation but may also facilitate prolonged oxidative gating. Together, these insights highlight TRPA1 activation signatures as predictors of allergen sensitising potency and provide a structural framework for evaluating chemical risk in ACD.

Importantly, TRPA1 activation by electrophiles cannot be separated from its role as a redox sensor. ROS such as hydrogen peroxide and lipid peroxidation products also activate TRPA1 via oxidation of the same cysteine cluster (Andersson et al., 2008; Trevisani et al., 2007). This dual sensitivity suggests a feed-forward mechanism: allergen binding initiates Ca^{2+} overload and mitochondrial stress, which generates ROS; in turn, ROS further oxidise TRPA1, prolonging channel activity. This synergy explains why *in vitro*, very low allergen concentrations-several orders of magnitude lower than those used *in vivo*-were sufficient to trigger strong cytotoxicity.

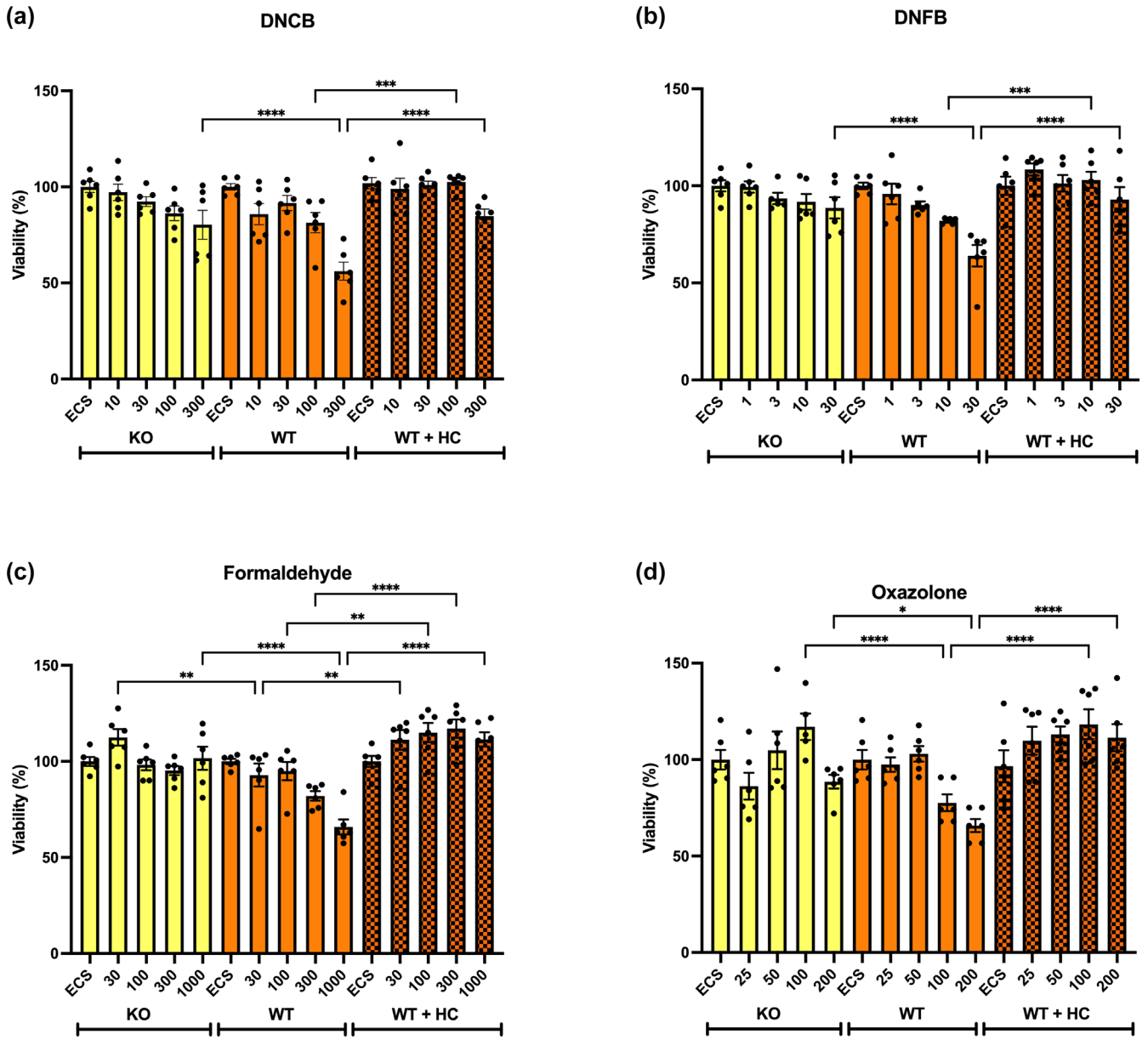

FIGURE 5 ATP luminescent cell viability assay in primary keratinocytes from wild-type (WT) and Trpa1 knockout (KO) mice following treatment with the contact sensitisers 2, 4-dinitrochlorobenzene (DNCB) (a), 2,4-dinitrofluorobenzene (DNFB) (b), formaldehyde (c) or oxazolone (d): Cell viability was assessed after exposure to increasing allergen concentrations to evaluate whether the effects on viability were mediated through TRPA1. Orange bars represent WT keratinocytes, yellow bars represent Trpa1 KO keratinocytes and patterned bars represent WT keratinocytes pretreated with the TRPA1 antagonist HC-030031 (HC). Allergen concentrations are shown in μM. ECS, extracellular solution, was used as a negative control. The TRPA1 agonist mustard oil (MO; 100 μM) was used as a positive control to validate assay specificity (see Figure S3). Data represent mean ± SEM of n = 6 biological replicates, each in technical triplicate. Statistical analysis was performed using one-way ANOVA with Šídák's post hoc test (**P < 0.0021, ***P < 0.0002, ****P < 0.0001).

An important consideration in this context is the marked disparity between the concentrations used *in vitro* and *in vivo*. In our assays, robust TRPA1 activation and keratinocyte cytotoxicity were observed at micromolar concentrations (e.g. 300-μM DNCB ≈0.006% w/v), whereas *in vivo* models typically employ 1%–2% solutions for sensitisation and 0.5%–2% for challenge. This represents a difference of 1,000-10,000-fold, suggesting that keratinocytes *in vivo* are exposed to overwhelming activation and cytotoxic stress. Within the adverse outcome pathway (AOP) framework for skin sensitisation, electrophiles are thought to deplete antioxidants and activate the **KEAP1–NRF2** pathway as an early key event (OECD, 2024; Yamaguchi et al., 2023). TRPA1, which harbours a cluster of redox-sensitive cysteines similar to KEAP1, may therefore operate in parallel or convergence with the NRF2 axis, acting as a complementary electrophile and ROS sensor. Our findings extend the adverse outcome pathway (AOP) concept by positioning TRPA1-dependent Ca^{2+} overload, cytotoxicity and IL-1α release as additional keratinocyte-driven key events that amplify downstream immune activation.

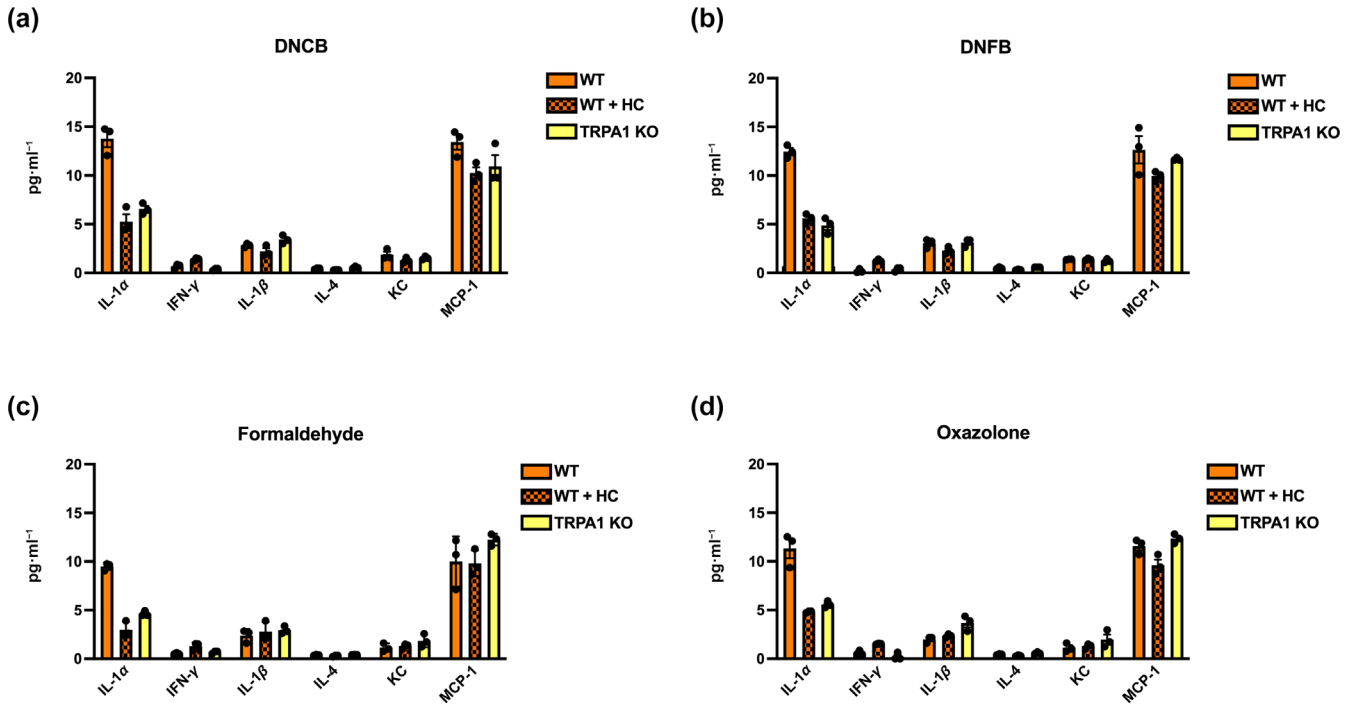

FIGURE 6 (a–d) Cytokine responses of keratinocytes following exposure to contact sensitisers. Primary murine keratinocytes were isolated from WT, WT were treated with the TRPA1 antagonist HC-030031, *Trpa1*$^{-/-}$ mice were exposed to contact sensitisers and cytokine levels were measured using multiplex Luminex analysis. IL-1α exhibited a TRPA1-dependent response pattern, whereas MCP-1 levels remained comparable between groups. Data are presented as scatter plots with mean ± SEM representing n = 3 independent biological replicates, each measured in technical duplicate. Due to the limited number of biological replicates and the exploratory nature of multiplex cytokine screening, statistical testing was not applied and results are presented descriptively.

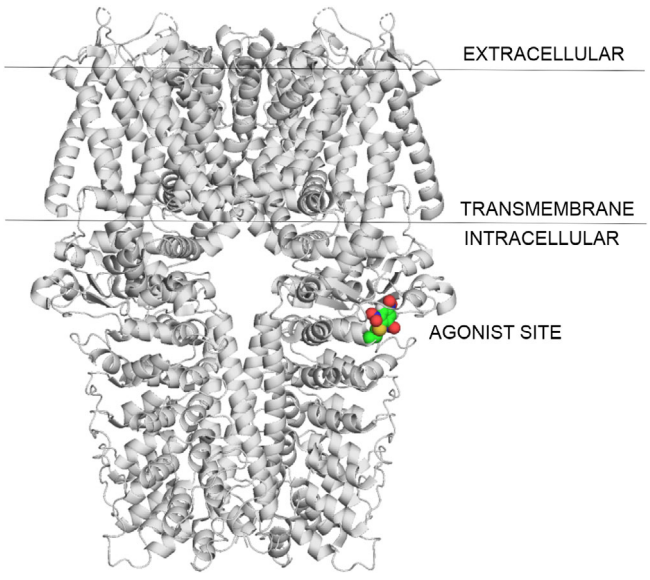

FIGURE 7 The human TRPA1 receptor (grey cartoon) in complex with 2, 4-dinitrochlorobenzene (DNCB) (spheres) in the nucleophilic agonist binding site.

Keratinocyte death and the selective release of IL-1α that we observed provide a mechanistic bridge to the adaptive immune phase. This concept is supported by recent findings showing that epithelial alarmin release functions as a decisive switch for immune amplification in barrier tissues (Mendoza et al., 2025). IL-1α is a prototypical alarmin, released from necrotic but not apoptotic cells, capable of recruiting and activating myeloid cells (Cohen et al., 2010; Di Paolo & Shayakhmetov, 2016). As a pre-formed alarmin, IL-1α can be passively released during keratinocyte injury, rendering partial persistence of IL-1α release following allergen exposure biologically plausible even when TRPA1 signalling is genetically or pharmacologically suppressed. This residual release is consistent with the contribution of TRPA1-independent cytotoxic stress pathways (Di Paolo & Shayakhmetov, 2016). In our multiplex cytokine measurements, IL-1α showed the clearest TRPA1-associated response pattern, with higher levels observed in WT keratinocytes compared with *Trpa1*$^{-/-}$ keratinocytes and reduced levels following pharmacological inhibition of TRPA1. Because these cytokine measurements were performed using a limited number of biological replicates (n = 3), the results should be interpreted as exploratory and hypothesis-generating and require confirmation in future studies with larger sample sizes. Thus, TRPA1-driven keratinocyte necrosis may serve as a decisive 'go' signal for dendritic cell migration and T-cell priming. This concept resonates with recent evidence that keratinocyte necroptosis is required for contact sensitisation to DNCB (Lian et al., 2022), suggesting that TRPA1-dependent cytotoxicity is not a bystander effect but a prerequisite for full sensitisation.

The mechanistic *in vitro* experiments presented here, including the exploratory multiplex cytokine measurements, were designed to

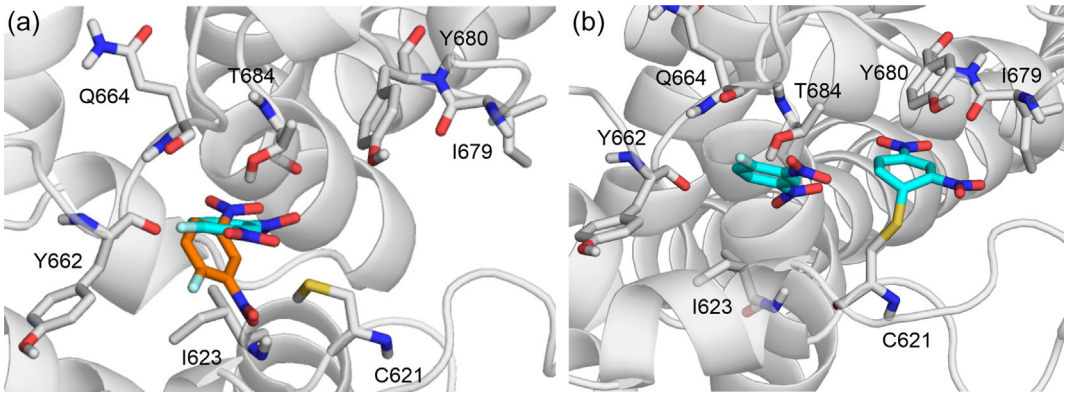

FIGURE 8 2, 4-dinitrofluorobenzene (DNFB) (teal sticks for Glide and orange sticks for FITTED) binding to the TRPA1 intracellular nucleophilic, agonist binding site in non-covalent and covalent binding modes. (a) The comparison of the Glide and FITTED non-covalent binding modes. (b) The comparison of Glide non-covalent and covalent binding modes. Interacting amino acids are labelled according to the numbering of protein data bank (PDB):6pqp and shown as grey sticks.

elucidate TRPA1-dependent epithelial responses and were therefore interpreted in the context of, and not independently from, the robust *in vivo* phenotype observed in the oxazolone-induced ACD model.

Together, our data also refine the division of labour between neuronal and non-neuronal TRPA1 in ACD. While neuronal TRPA1 mediates acute itch and neurogenic inflammation (Feng et al., 2017; Liu et al., 2013), keratinocyte TRPA1 emerges here as a driver of cytotoxicity and alarmin release. Moreover, environmental exposures such as the phthalate plasticizer diisononyl phthalate (DINP) can exacerbate ACD by upregulating TRPA1 expression, an effect preventable by TRPA1 antagonism (Kang et al., 2017). These observations support a cooperative model in which neuronal TRPA1 propagates sensory and vascular responses, whereas keratinocyte TRPA1 initiates an epithelial danger programme that ultimately fuels adaptive immune activation.

From a translational standpoint, the observation that TRPA1 antagonism rescues keratinocytes from cytotoxic injury is highly relevant. More broadly, strategies that target epithelial danger sensors align with recent insights showing that modulation of epithelial alarmin release can recalibrate immune responses in inflammatory skin disease (Mendoza et al., 2025). By interrupting both axes of activation, electrophilic binding and ROS amplification, antagonists such as HC-030031 prevent IL-1α release and limit inflammation. Similar protective effects of TRPA1 antagonism have also been demonstrated in cutaneous injury models induced by reactive chemicals such as tear gas (Achanta et al., 2024). This dual protective effect suggests TRPA1 blockade as a rational therapeutic strategy in ACD, particularly for strong sensitisers where cytotoxic stress is most pronounced. Beyond therapy, the allergen-TRPA1 binding profile itself may serve as a predictor of sensitisation potency, offering a novel parameter for risk assessment of chemical allergens.

4.1 | Clinical implications and future directions

Our findings place keratinocyte TRPA1 at the centre of the early danger responses that shape ACD. By demonstrating that TRPA1 integrates direct electrophilic binding with ROS amplification, we identify the channel as a crucial amplifier of keratinocyte cytotoxicity and IL-1α release. This dual mechanism underscores the therapeutic promise of TRPA1 antagonists such as HC-030031, which can interrupt both axes of activation to preserve epidermal integrity and limit downstream inflammation. Beyond therapy, IL-1α emerges as a potential surrogate marker of TRPA1 activity in keratinocytes, offering translational value for both diagnostics and risk assessment.

Future studies should refine the mechanistic basis of allergen–TRPA1 interactions in live tissue, for example using TRPA1 A-loop mutants to dissect structure–activity relationships *in situ*. Investigations into repeated or chronic exposures are also warranted, as the cumulative effects of electrophilic allergens may differ from acute responses. Importantly, patient-specific expression patterns of keratinocyte TRPA1, revealed by RNAscope, call for further exploration in human ACD and chronic dermatitis subtypes, where interindividual variability could inform personalised therapeutic strategies.

4.2 | Conclusion

Taken together, our integrated *in vitro*, *in vivo* and *in silico* analyses establish keratinocyte TRPA1 as a critical sensor and effector in the pathogenesis of allergic contact dermatitis (ACD). By linking allergen binding modes to cytotoxicity, ROS amplification and IL-1α release, we show that keratinocyte TRPA1 activity is not merely a bystander phenomenon but a driver of epidermal damage and immune amplification. Pharmacological antagonism of TRPA1 effectively rescued keratinocytes from allergen-induced injury, highlighting a therapeutic avenue for disease prevention or mitigation. More broadly, the structural and functional insights into allergen-TRPA1 interactions provide a framework for predicting sensitising potency and guiding the design of safer compounds with reduced allergenic potential, thereby extending the understanding of TRPA1 biology beyond its established role in sensory neurons.

AUTHOR CONTRIBUTIONS

Areej Jaber: Methodology; investigation; conceptualization; formal analysis; validation; visualization; writing—original draft; writing—review and editing. **Szabina Horváth:** Investigation. **Balázs Zoltán Zsidó:** Investigation. **Viktória Kormos:** Funding acquisition; investigation; writing—review and editing. **János Konkoly:** Investigation. **Csaba Hetényi:** Investigation; funding acquisition; writing—review and editing. **Erika Pintér:** Conceptualization; resources; writing—review and editing; funding acquisition; visualization; supervision; project administration; methodology. **Ágnes Kemény:** Supervision; visualization; writing—review and editing; conceptualization; methodology; project administration; formal analysis. **Rolland Gyulai:** Conceptualization; supervision; resources; funding acquisition; writing—review and editing; visualization; project administration.

ACKNOWLEDGEMENTS

We acknowledge the Digital Government Development and Project Management Ltd. for awarding us access to the Komondor HPC facility based in Hungary.

ChatGPT (OpenAI, San Francisco, CA) was used to assist with English language editing and reference mining, and BioRender (https://BioRender.com) was used for graphical abstract drafting and figure creation. All scientific content, analyses and conclusions were generated and validated by the authors.

CONFLICT OF INTEREST STATEMENT

The authors declare no conflicts of interest.

DATA AVAILABILITY STATEMENT

The data that support the findings of this study are available from the corresponding author on reasonable request. Raw figure data will be retained for at least 10 years in accordance with the *British Journal of Pharmacology* data-retention policy.

DECLARATION OF TRANSPARENCY AND SCIENTIFIC RIGOUR

This Declaration acknowledges that this paper adheres to the principles for transparent reporting and scientific rigour of preclinical research as stated in the *BJP* guidelines for Design & Analysis, Immunoblotting and Immunochemistry, and Animal Experimentation and as recommended by funding agencies, publishers and other organizations engaged with supporting research. The authors confirm that the study design, data collection, analysis and reporting were conducted to minimise bias and ensure reproducibility.

REFERENCES

Achanta, S., Chintagari, N. R., Balakrishna, S., Liu, B., & Jordt, S.-E. (2024). Pharmacologic inhibition of transient receptor potential Ion Channel Ankyrin 1 counteracts 2-Chlorobenzalmalononitrile tear gas agent–induced cutaneous injuries. *The Journal of Pharmacology and Experimental Therapeutics*, *388*(2), 613–623. https://doi.org/10.1124/jpet.123.001666

Alexander, S. P. H., Fabbro, D., Peach, C. J., Gibb, A. J., Kelly, E., Mathie, A. A., Veale, E. L., Armstrong, J. F., Faccenda, E., Harding, S. D., Southan, C., Davies, J. A., Beuve, A., Brouckaert, P., Bryant, C., Burnett, J. C., Farndale, R. W., Friebe, A., Garthwaite, J., … Waldman, S. A. (2025). The concise guide to pharmacology 2025/26: Catalytic receptors. *British Journal of Pharmacology*, *182*(Suppl 1), S259–S306. https://doi.org/10.1111/bph.70233

Alexander, S. P. H., Roberts, R. E., Broughton, B. R. S., Sobey, C. G., George, C. H., Stanford, S. C., Cirino, G., Docherty, J. R., Giembycz, M. A., Hoyer, D., Insel, P. A., Izzo, A. A., Ji, Y., MacEwan, D. J., Mangum, J., Wonnacott, S., & Ahluwalia, A. (2018). Goals and practicalities of immunoblotting and immunohistochemistry: A guide for submission to the *British Journal of Pharmacology*. *British Journal of Pharmacology*, *175*, 407–411. https://doi.org/10.1111/bph.14112

Alexander, S. P. H., Striessnig, J., Gibb, A. J., Mathie, A. A., Veale, E. L., Kelly, E., Peach, C. J., Armstrong, J. F., Faccenda, E., Harding, S. D., Southan, C., Davies, J. A., Aldrich, R. W., Attali, B., Baggetta, A. M., Becirovic, E., Beech, D. J., Biel, M., Bill, R. M., … Zhu, M. (2025). The concise guide to pharmacology 2025/26: Ion channels. *British Journal of Pharmacology*, *182*(Suppl. 1), S152–S241. https://doi.org/10.1111/bph.70231

Andersson, D. A., Gentry, C., Moss, S., & Bevan, S. (2008). Transient receptor potential A1 is a sensory receptor for multiple products of oxidative stress. *The Journal of Neuroscience*, *28*(10), 2485–2494. https://doi.org/10.1523/JNEUROSCI.5369-07.2008

Atoyan, R., Shander, D., & Botchkareva, N. V. (2009). Non-neuronal expression of transient receptor potential type A1 (TRPA1) in human skin. *Journal of Investigative Dermatology*, *129*(9), 2312–2315. https://doi.org/10.1038/jid.2009.58

Banki, E., Hajna, Z., Kemeny, A., Botz, B., Nagy, P., Bolcskei, K., Toth, G., Reglodi, D., & Helyes, Z. (2014). The selective PAC1 receptor agonist maxadilan inhibits neurogenic vasodilation and edema formation in the mouse skin. *Neuropharmacology*, *85*, 538–547. https://doi.org/10.1016/j.neuropharm.2014.06.019

Bánvölgyi, Á., Pálinkás, L., Berki, T., Clark, N., Grant, A. D., Helyes, Z., Pozsgai, G., Szolcsányi, J., Brain, S. D., & Pintér, E. (2005). Evidence for a novel protective role of the vanilloid TRPV1 receptor in a cutaneous contact allergic dermatitis model. *Journal of Neuroimmunology*, *169*(1–2), 86–96. https://doi.org/10.1016/j.jneuroim.2005.08.012

Bautista, D. M., Jordt, S.-E., Nikai, T., Tsuruda, P. R., Read, A. J., Poblete, J., Yamoah, E. N., Basbaum, A. I., & Julius, D. (2006). TRPA1 mediates the inflammatory actions of environmental irritants and Proalgesic agents. *Cell*, *124*(6), 1269–1282. https://doi.org/10.1016/j.cell.2006.02.023

Bautista, D. M., Pellegrino, M., & Tsunozaki, M. (2013). TRPA1: A gatekeeper for inflammation. *Annual Review of Physiology*, *75*(1), 181–200. https://doi.org/10.1146/annurev-physiol-030212-183811

Berman, H. M. (2000). The protein data bank. *Nucleic Acids Research*, *28*(1), 235–242. https://doi.org/10.1093/nar/28.1.235

Brites, G. S., Ferreira, I., Sebastião, A. I., Silva, A., Carrascal, M., Neves, B. M., & Cruz, M. T. (2020). Allergic contact dermatitis: From pathophysiology to development of new preventive strategies. *Pharmacological Research*, *162*, 105282. https://doi.org/10.1016/j.phrs.2020.105282

Brys, A. K., Rodriguez-Homs, L. G., Suwanpradid, J., Atwater, A. R., & MacLeod, A. S. (2020). Shifting paradigms in allergic contact dermatitis: The role of innate immunity. *Journal of Investigative Dermatology*, *140*(1), 21–28. https://doi.org/10.1016/j.jid.2019.03.1133

Cohen, I., Rider, P., Carmi, Y., Braiman, A., Dotan, S., White, M. R., Voronov, E., Martin, M. U., Dinarello, C. A., & Apte, R. N. (2010). Differential release of chromatin-bound IL-1α discriminates between necrotic and apoptotic cell death by the ability to induce sterile inflammation. *Proceedings of the National Academy of Sciences*, *107*(6), 2574–2579. https://doi.org/10.1073/pnas.0915018107

Corbeil, C. R., Englebienne, P., & Moitessier, N. (2007). Docking ligands into flexible and solvated macromolecules. 1. Development and validation of FITTED 1.0. *Journal of Chemical Information and Modeling*, *47*(2), 435–449. https://doi.org/10.1021/ci6002637

Curtis, M. J., Alexander, S. P. H., Cortese-Krott, M., Kendall, D. A., Martemyanov, K. A., Mauro, C., Panettieri, R. A. Jr., Papapetropoulos, A., Patel, H. H., Santo, E. E., Schulz, R., Stefanska, B., Stephens, G. J., Teixeira, M. M., Vergnolle, N., Wang, X., & Ferdinandy, P. (2025). Guidance on the planning and reporting of experimental design and analysis. *British Journal of Pharmacology*, *182*, 1413–1415. https://doi.org/10.1111/bph.17441

Das, P., Mounika, P., Yellurkar, M. L., Prasanna, V. S., Sarkar, S., Velayutham, R., & Arumugam, S. (2022). Keratinocytes: An enigmatic factor in atopic dermatitis. *Cells*, *11*(10), 1683. https://doi.org/10.3390/cells11101683

Dhingra, N., Shemer, A., Correa da Rosa, J., Rozenblit, M., Fuentes-Duculan, J., Gittler, J. K., Finney, R., Czarnowicki, T., Zheng, X., Xu, H., Estrada, Y. D., Cardinale, I., Suárez-Fariñas, M., Krueger, J. G., & Guttman-Yassky, E. (2014). Molecular profiling of contact dermatitis skin identifies allergen-dependent differences in immune response. *Journal of Allergy and Clinical Immunology*, *134*(2), 362–372. https://doi.org/10.1016/j.jaci.2014.03.009

Di Paolo, N. C., & Shayakhmetov, D. M. (2016). Interleukin 1α and the inflammatory process. *Nature Immunology*, *17*(8), 906–913. https://doi.org/10.1038/ni.3503

Feng, J., Yang, P., Mack, M. R., Dryn, D., Luo, J., Gong, X., Liu, S., Oetjen, L. K., Zholos, A. V., Mei, Z., Yin, S., Kim, B. S., & Hu, H. (2017). Sensory TRP channels contribute differentially to skin inflammation and persistent itch. *Nature Communications*, *8*(1), 980. https://doi.org/10.1038/s41467-017-01056-8

Friesner, R. A., Banks, J. L., Murphy, R. B., Halgren, T. A., Klicic, J. J., Mainz, D. T., Repasky, M. P., Knoll, E. H., Shelley, M., Perry, J. K., Shaw, D. E., Francis, P., & Shenkin, P. S. (2004). Glide: A new approach for rapid, accurate docking and scoring. 1. Method and assessment of docking accuracy. *Journal of Medicinal Chemistry*, *47*(7), 1739–1749. https://doi.org/10.1021/jm0306430

Gaspari, A. A. (1997). The role of keratinocytes in the pathophysiology of contact dermatitis. *Immunology and Allergy Clinics of North America*, *17*(3), 377–405. https://doi.org/10.1016/S0889-8561(05)70316-7

Gilliver, S. C., Ashworth, J. J., & Ashcroft, G. S. (2007). The hormonal regulation of cutaneous wound healing. *Clinics in Dermatology*, *25*(1), 56–62. https://doi.org/10.1016/j.clindermatol.2006.09.012

Honda, T., Egawa, G., Grabbe, S., & Kabashima, K. (2013). Update of immune events in the murine contact hypersensitivity model: Toward the understanding of allergic contact dermatitis. *Journal of Investigative Dermatology*, *133*(2), 303–315. https://doi.org/10.1038/jid.2012.284

Kang, J., Ding, Y., Li, B., Liu, H., Yang, X., & Chen, M. (2017). TRPA1 mediated aggravation of allergic contact dermatitis induced by DINP and regulated by NF-κB activation. *Scientific Reports*, *7*(1), 43586. https://doi.org/10.1038/srep43586

King, D. T. (1979). Munro microabscess: Let's spell it right. *Archives of Dermatology*, *115*(7), 816. https://doi.org/10.1001/archderm.1979.04010070002004

Landini, L., de Souza Monteiro Araujo, D., Titiz, M., Geppetti, P., Nassini, R., & De Logu, F. (2022). TRPA1 role in inflammatory disorders: What is known so far? *International Journal of Molecular Sciences*, *23*(9), 4529. https://doi.org/10.3390/ijms23094529

Li, F., Adase, C. A., & Zhang, L. (2017). Isolation and culture of primary mouse keratinocytes from neonatal and adult mouse skin. *Journal of Visualized Experiments*, *125*, e56027. https://doi.org/10.3791/56027

Lian, N., Chen, Y., Chen, S., Xiao, T., Song, C., Ke, Y., Wei, X., Gong, C., Yu, H., Gu, H., Chen, Q., Li, M., & Chen, X. (2022). Necroptosis-mediated HMGB1 secretion of keratinocytes as a key step for inflammation development in contact hypersensitivity. *Cell Death Discovery*, *8*(1), 451. https://doi.org/10.1038/s41420-022-01228-6

Lilley, E., Stanford, S. C., Kendall, D. E., Alexander, S. P. H., Cirino, G., Docherty, J. R., George, C. H., Insel, P. A., Izzo, A. A., Ji, Y., Panettieri, R. A., Sobey, C. G., Stefanska, B., Stephens, G., Teixeira, M., & Ahluwalia, A. (2020). ARRIVE 2.0 and the British Journal of Pharmacology: Updated guidance for 2020. *British Journal of Pharmacology*, *177*(16), 3611–3616. https://doi.org/10.1111/BPH.15178

Liu, B., Escalera, J., Balakrishna, S., Fan, L., Caceres, A. I., Robinson, E., Sui, A., McKay, M. C., McAlexander, M. A., Herrick, C. A., & Jordt, S. E. (2013). TRPA1 controls inflammation and pruritogen responses in allergic contact dermatitis. *The FASEB Journal*, *27*(9), 3549–3563. https://doi.org/10.1096/fj.13-229948

Lv, J., Zou, L., Zhao, L., Yang, W., Xiong, Y., Li, B., & He, R. (2015). Leukotriene B 4—Leukotriene B 4 receptor axis promotes oxazolone-induced contact dermatitis by directing skin homing of neutrophils and CD 8+ T cells. *Immunology*, *146*(1), 50–58. https://doi.org/10.1111/imm.12478

Ma, H., Shu, Q., Li, Z., Song, X., & Xu, H. (2023). Formaldehyde aggravates allergic contact dermatitis by facilitating NLRP3 inflammasome activation in macrophages. *International Immunopharmacology*, *117*, 109904. https://doi.org/10.1016/j.intimp.2023.109904

Macpherson, L. J., Dubin, A. E., Evans, M. J., Marr, F., Schultz, P. G., Cravatt, B. F., & Patapoutian, A. (2007). Noxious compounds activate TRPA1 ion channels through covalent modification of cysteines. *Nature*, *445*(7127), 541–545. https://doi.org/10.1038/nature05544

Mäki-Opas, I., Hämäläinen, M., Moilanen, L. J., Sood, H., Leppänen, T., Kummola, L., Junttila, I. S., Lehtimäki, L., & Moilanen, E. (2023). TRPA1 mediates contact hypersensitivity induced by 2,4-dinitrochlorobenzene. *Journal of Investigative Dermatology*, *143*(6), 1104–1108.e4. https://doi.org/10.1016/j.jid.2022.12.014

Martinov, T., Glenn-Finer, R., Burley, S., Tonc, E., Balsells, E., Ashbaugh, A., Swanson, L., Daughters, R. S., & Chatterjea, D. (2013). Contact hypersensitivity to Oxazolone provokes vulvar mechanical hyperalgesia in mice. *PLoS ONE*, *8*(10), e78673. https://doi.org/10.1371/journal.pone.0078673

Mendoza, A., Bou-Puerto, R., Jara, J. S., Dikiy, S., Giovanelli, P., Correa, D., Manenti, S., Andretta, E. S., Dahia, C. L., & Rudensky, A. Y. (2025). Enkephalin-producing regulatory T cells in the skin restrain local inflammation through control of nociception. *Science Immunology*, *10*(111), adz6869. https://doi.org/10.1126/sciimmunol.adz6869

Moilanen, L. J., Laavola, M., Kukkonen, M., Korhonen, R., Leppänen, T., Högestätt, E. D., Zygmunt, P. M., Nieminen, R. M., & Moilanen, E. (2012). TRPA1 contributes to the acute inflammatory response and mediates carrageenan-induced paw edema in the mouse. *Scientific Reports*, *2*(1), 380. https://doi.org/10.1038/srep00380

Moyle, M., Cevikbas, F., Harden, J. L., & Guttman-Yassky, E. (2019). Understanding the immune landscape in atopic dermatitis: The era of biologics and emerging therapeutic approaches. *Experimental Dermatology*, *28*(7), 756–768. https://doi.org/10.1111/exd.13911

OECD. (2024). Test No. 442D: In Vitro Skin Sensitisation, https://doi.org/10.1787/9789264229822-en

Paulsen, C. E., Armache, J.-P., Gao, Y., Cheng, Y., & Julius, D. (2015). Structure of the TRPA1 ion channel suggests regulatory mechanisms. *Nature*, *520*(7548), 511–517. https://doi.org/10.1038/nature14367

Percie du Sert, N., Hurst, V., Ahluwalia, A., Alam, S., Avey, M. T., Baker, M., Browne, W. J., Clark, A., Cuthill, I. C., Dirnagl, U., Emerson, M., Garner, P., Holgate, S. T., Howells, D. W., Karp, N. A., Lazic, S. E., Lidster, K., MacCallum, C. J., Macleod, M., … Würbel, H. (2020). The ARRIVE guidelines 2.0: updated guidelines for reporting animal research. *PLoS Biology*, *18*(7), e3000410. https://doi.org/10.1371/journal.pbio.3000410

Pozsgai, G., Hajna, Z., Bagoly, T., Boros, M., Kemény, Á., Materazzi, S., Nassini, R., Helyes, Z., Szolcsányi, J., & Pintér, E. (2012). The role of transient receptor potential ankyrin 1 (TRPA1) receptor activation in hydrogen-sulphide-induced CGRP-release and vasodilation. *European Journal of Pharmacology*, *689*(1–3), 56–64. https://doi.org/10.1016/j.ejphar.2012.05.053

Pozsgai, G., Payrits, M., Sághy, É., Sebestyén-Bátai, R., Steen, E., Szőke, É., Sándor, Z., Solymár, M., Garami, A., Orvos, P., Tálosi, L., Helyes, Z., & Pintér, E. (2017). Analgesic effect of dimethyl trisulfide in mice is mediated by TRPA1 and sst 4 receptors. *Nitric Oxide*, *65*, 10–21. https://doi.org/10.1016/j.niox.2017.01.012

Schrödinger, L. (2024). Schrödinger Release 2024–1: Maestro (No. 2024–1), Schrödinger, LLC

Suo, Y., Wang, Z., Zubcevic, L., Hsu, A. L., He, Q., Borgnia, M. J., Ji, R.-R., & Lee, S.-Y. (2020). Structural insights into electrophile irritant sensing by the human TRPA1 channel. *Neuron*, *105*(5), 882–894.e5. https://doi.org/10.1016/j.neuron.2019.11.023

Therrien, E., Weill, N., Tomberg, A., Corbeil, C. R., Lee, D., & Moitessier, N. (2014). Docking ligands into flexible and solvated macromolecules. 7. Impact of protein flexibility and water molecules on docking-based virtual screening accuracy. *Journal of Chemical Information and Modeling*, *54*(11), 3198–3210. https://doi.org/10.1021/ci500299h

Trevisani, M., Siemens, J., Materazzi, S., Bautista, D. M., Nassini, R., Campi, B., Imamachi, N., Andrè, E., Patacchini, R., Cottrell, G. S., Gatti, R., Basbaum, A. I., Bunnett, N. W., Julius, D., & Geppetti, P. (2007). 4-Hydroxynonenal, an endogenous aldehyde, causes pain and neurogenic inflammation through activation of the irritant receptor TRPA1. *Proceedings of the National Academy of Sciences*, *104*(33), 13519–13524. https://doi.org/10.1073/pnas.0705923104

Tuckermann, J. P., Kleiman, A., Moriggl, R., Spanbroek, R., Neumann, A., Illing, A., Clausen, B. E., Stride, B., Förster, I., Habenicht, A. J. R., Reichardt, H. M., Tronche, F., Schmid, W., & Schütz, G. (2007). Macrophages and neutrophils are the targets for immune suppression by glucocorticoids in contact allergy. *Journal of Clinical Investigation*, *117*(5), 1381–1390. https://doi.org/10.1172/JCI28034

Uribe-Herranz, M., Lian, L.-H., Hooper, K. M., Milora, K. A., & Jensen, L. E. (2013). IL-1R1 signaling facilitates Munro's microabscess formation in Psoriasiform Imiquimod-induced skin inflammation. *Journal of Investigative Dermatology*, *133*(6), 1541–1549. https://doi.org/10.1038/jid.2012.512

Van Der Spoel, D., Lindahl, E., Hess, B., Groenhof, G., Mark, A. E., & Berendsen, H. J. C. (2005). GROMACS: Fast, flexible, and free. *Journal of Computational Chemistry*, *26*(16), 1701–1718. https://doi.org/10.1002/jcc.20291

Voskuhl, R. (2011). Sex differences in autoimmune diseases. *Biology of Sex Differences*, *2*(1), 1. https://doi.org/10.1186/2042-6410-2-1

Wang, F., Flanagan, J., Su, N., Wang, L.-C., Bui, S., Nielson, A., Wu, X., Vo, H.-T., Ma, X.-J., & Luo, Y. (2012). RNAscope: A novel in situ RNA analysis platform for formalin-fixed, paraffin-embedded tissues. *The Journal of Molecular Diagnostics: JMD*, *14*(1), 22–29. https://doi.org/10.1016/j.jmoldx.2011.08.002

Waterhouse, A., Bertoni, M., Bienert, S., Studer, G., Tauriello, G., Gumienny, R., Heer, F. T., de Beer, T. A. P., Rempfer, C., Bordoli, L., Lepore, R., & Schwede, T. (2018). SWISS-MODEL: Homology modelling of protein structures and complexes. *Nucleic Acids Research*, *46*(W1), W296–W303. https://doi.org/10.1093/nar/gky427

Yamaguchi, H. L., Yamaguchi, Y., & Peeva, E. (2023). Role of innate immunity in allergic contact dermatitis: An update. *International Journal of Molecular Sciences*, *24*(16), 12975. https://doi.org/10.3390/ijms241612975

Ye, J., & Lai, Y. (2025). Keratinocytes: New perspectives in inflammatory skin diseases. *Trends in Molecular Medicine*, *31*, 1103–1113. https://doi.org/10.1016/j.molmed.2025.03.012

Zsidó, B. Z., Börzsei, R., Pintér, E., & Hetényi, C. (2021). Prerequisite binding modes determine the dynamics of action of covalent agonists of ion channel TRPA1. *Pharmaceuticals*, *14*(10), 988. https://doi.org/10.3390/ph14100988

SUPPORTING INFORMATION

Additional supporting information can be found online in the Supporting Information section at the end of this article.

How to cite this article: Jaber, A., Horváth, S., Zsidó, B. Z., Kormos, V., Konkoly, J., Hetényi, C., Pintér, E., Kemény, Á., & Gyulai, R. (2026). Contact sensitisers activate keratinocytes and induce cytotoxicity via Transient Receptor Potential Ankyrin 1 in allergic contact dermatitis. *British Journal of Pharmacology*, 1–18. https://doi.org/10.1111/bph.70479